# Electrically widely tunable interband cascade lasers

Yuchao Jiang,[1] Lu Li,[1] Zhaobing Tian,[1] Hao Ye,[1] Lihua Zhao,[1] Rui Q. Yang,[1]
Tetsuya D. Mishima,[2] Michael B. Santos,[2] Matthew B. Johnson,[2] and Kamjou Mansour[3]
[1]*School of Electrical and Computer Engineering, University of Oklahoma, Norman, Oklahoma 73019, USA*
[2]*Homer L. Dodge Department of Physics and Astronomy, University of Oklahoma, Norman, Oklahoma 73019, USA*
[3]*Jet Propulsion Laboratory, California Institute of Technology, Pasadena, California 91109, USA*

(Received 12 December 2013; accepted 28 January 2014; published online 18 March 2014)

Electrically tunable interband cascade lasers are demonstrated with a wide tuning range of about 280 $cm^{-1}$ (34 meV in energy or 630 nm in wavelength) near 4.5 $\mu$m and about 180 $cm^{-1}$ (22 meV or 900 nm) near 7 $\mu$m wavelengths. The laser structures are designed such that the heating and Stark effects act together to enhance the red-shift of the lasing wavelength with current injection to achieve wide tunability. The control and manipulation of the tuning range and rate are discussed. © *2014 AIP Publishing LLC*. [http://dx.doi.org/10.1063/1.4865941]

## I. INTRODUCTION

Semiconductor mid-infrared (IR) lasers with a wide tuning range are highly desirable for many applications such as spectroscopy and biochemical analysis.[1] Tunable quantum cascade (QC) lasers have been pursued from their early stages.[2] Several approaches have been applied to QC lasers, including: single-mode distributed feedback (DFB) lasers,[3] two-section lasers,[4] heterogeneous active regions,[5] and external cavities (ECs).[6] Each approach has shortcomings. For example, DFB lasers can produce single-mode emission but have a very limited current-controlled tuning range (~10 $cm^{-1}$). Multi-section lasers with parallel and independent current injection for each section, through multiple contacts, can have a large tuning range, but have higher threshold current and require extra device fabrication steps. And EC lasers lack long term mechanical and vibrational stability and require well-aligned external optics components. For convenience and simplicity, it is desirable to have a monolithic laser architecture with a wide tuning range through an electric current injection without extra fabrication complications and additional external parts. Recently, QC lasers with a relatively large tuning range (e.g., 80 $cm^{-1}$) through varying voltage were reported.[7,8]

For interband cascade (IC) lasers,[9] however, not much effort has been devoted to achieving wide tuning capability although continuous wave (cw) operation at room temperature and above has been demonstrated with record-low electrical power consumption among all mid-IR semiconductor laser architectures.[10,11] Compared with QC lasers, IC lasers exhibit some unique properties that turn out to be more suitable for making widely tunable mid-IR sources. First, the gain width of an interband transition is inherently much broader than that of an intersubband transition. Second, the transition energy (or the bandgap) of an IC laser decreases with rising temperature and has a larger temperature coefficient than that of the intersubband transition energy of a QC laser (e.g., ~−1.0 $cm^{-1}$/K for IC lasers[12] and ~−0.47 $cm^{-1}$/K for QC lasers[13] both emitting at 4.3 $\mu$m). Hence heat generated by either temperature change or current Joule heating in the laser active region can be used more effectively for tuning the lasing wavelength in IC lasers. In addition, the spatially indirect transition in the type-II quantum well (QW) active region allows a large nonzero dipole moment similar to a diagonal transition in a QC laser. Consequently, a strong first-order Stark effect can be used to tune the emission wavelength in an IC laser by an electric field. Thus, with a proper design, such properties can be used collectively in an IC laser to generate a wide tuning range. To date, there has been only one attempt reported on electrically tunable IC lasers with a tuning range of 120 $cm^{-1}$ (15 meV in energy or 120 nm in wavelength) near 3.3 $\mu$m (at 80 K) based on a single-pair InAs/GaInSb type-II QW active region.[14] In this paper, we demonstrate electrically tunable IC lasers with a tuning range of about 280 $cm^{-1}$ (34 meV in energy or 630 nm in wavelength) near 4.5 $\mu$m and about 180 $cm^{-1}$ (22 meV or 900 nm) near 7 $\mu$m. Also, different active region structures are explored for manipulating the tuning rate and range.

## II. TUNABLE IC LASER STRUCTURES AND EXPERIMENTAL RESULTS

The active region of an IC laser usually consists of a W-like QW (Ref. 15) that has one GaInSb layer sandwiched by two InAs layers surrounded by AlSb confinement layers, as shown in Fig. 1. The wave-function modulus profiles for the ground state of the electron and heavy hole, which were calculated using a two-band model,[17] are also shown in Fig. 1. The bandgap of the active region ($E_g$) is the energy difference between the electron and hole ground states ($E_e$-$E_h$), which determines the emitted photon energy ($h\nu$) and thus the lasing wavelength $\lambda$. In operation, a forward bias voltage is applied to the device, resulting in an electric filed, $F$, along the direction from right to left in Fig. 1. Consequently, the bandgap ($E_g$) will change with the electric field ($F$) according to Stark effect. The Stark shift, the energy change of such an interband transition ($\Delta E$) in type-II QWs, can be written as[2]

$$\Delta E = -q|\Delta F|\ (z_e - z_h), \tag{1}$$

 

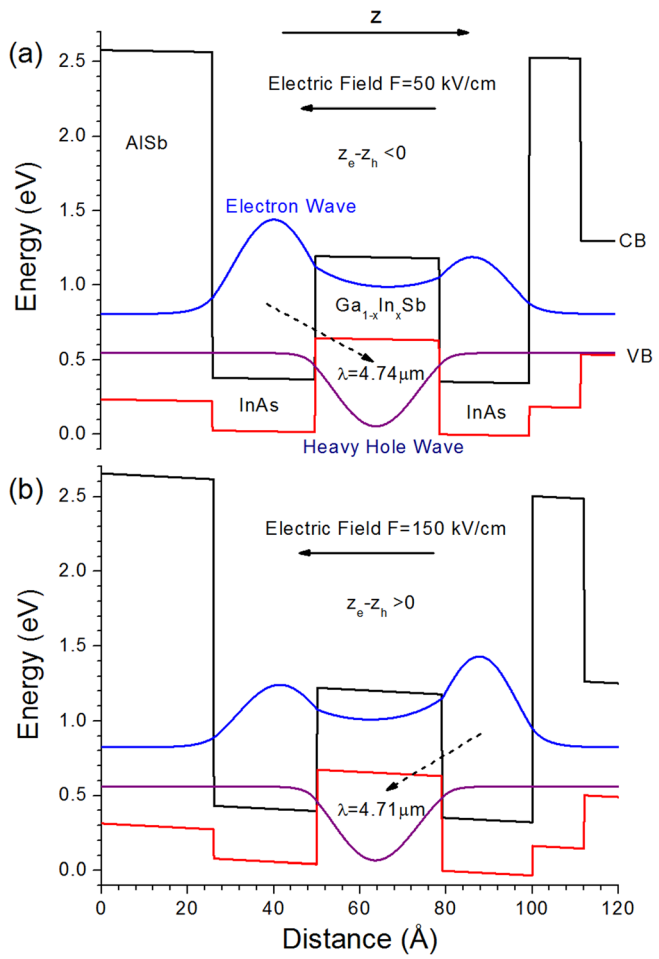


FIG. 1. Moduli profiles of the envelope functions for electrons and holes in the "W" active region for different electric fields. The direction of electric field is from right to left while the direction of displacement is from left to right. Dashed arrows indicate the transitions related to lasing.

where $q$ is the electron charge, $\Delta F$ is an increment increase of the electric field, $F$, across the active region, ($z_e$-$z_h$) is the distance between the centroids of the electron and hole probability distributions, and the minus sign is because the electric field is in the opposite direction of z. Depending on whether the electron state is mainly on the left (Fig. 1(a)) or right (Fig. 1(b)) InAs layer, the value of the interband dipole ($z_e$-$z_h$) can be either negative or positive and consequently the emission wavelength would have a blue-shift or a red-shift, respectively, with increasing electric field according to Eq. (1). The latter is of particular interest in this work because it can be combined with temperature tuning to achieve a large tuning range.

Whether the electron distribution is mainly in the left or right InAs layer can be manipulated by adjusting the two InAs layer thicknesses in the active region and by changing the electric field with the applied voltage across the laser structure. In the past, the active regions of most IC lasers and emitters were designed with the electron distribution mainly located on the left-side InAs layer or without the right-side InAs layer,[14,16] resulting in the blue-shift of emission wavelength with the applied bias voltage.[14,16] However, a large electric field can switch the electron distribution from the left-side InAs layer initially to the right-side InAs layer. This is illustrated in Fig. 1 for a typical W-shape active region where the electron wave-function is distributed more on the right InAs layer as the electric field increases, while the heavy-hole wave-function is almost unchanged. Once the centroid of the electron wave-function is on the right side of the hole wave-function, the value of ($z_e$-$z_h$) becomes positive and the interband transition energy will decrease with a further increase of the forward bias voltage. Hence, the sign of the interband dipole ($z_e$-$z_h$) decides the emission wavelength's shifting direction (red or blue), while the magnitude of ($z_e$-$z_h$) determines the wavelength tuning rate and range with the electric field according to Eq. (1). These properties of the interband dipole ($z_e$-$z_h$) are closely related to electron and hole wave-functions in the active region, which will be exploited in this work by varying the QW structures in the active region. In subsection II A, studies of a set of IC lasers with two InAs QW layer structures in the active region will be presented. In subsection II B, IC lasers with three InAs QW layers in the active region will be described. Also, how the carrier concentration pinning at the threshold may be unlocked, which is related to lasing wavelength tuning, will be discussed.

### A. IC lasers with two InAs QW layers in the active region

A series of IC laser structures, labeled R066, R084, R089, and R090, were designed with different thicknesses for the InAs QW layers in their active regions, resulting in variations of electron distribution in their corresponding InAs layers. As shown in Table I, the layer thicknesses of the InAs/$Ga_{0.7}In_{0.3}Sb$/InAs QWs in the active region (in Å from left to right) for R066, R084, R089, and R090 are 24/29/21, 22/29/21, 22/29/23, and 22/29/21, respectively. The active region of R090 has an additional $Ga_{0.7}In_{0.3}Sb$ layer of 29 Å on the right. R066 has 12 cascade stages, while the other structures have 8 cascade stages. The laser structures were grown using a Gen-II molecular beam epitaxy (MBE) system on $n^+$-doped InAs substrates. The injection region and waveguide structures are similar to ones described in Ref. 18.

After growth, the wafers were processed into 150-$\mu$m-wide broad-area and narrow-ridge (width: 10 to 40 $\mu$m) waveguide laser devices with both facets uncoated and mounted epi-side up on copper heat-sinks for measurements. The optical output power of the fabricated lasers was measured by a thermopile power meter for cw operation. A Nicolet Fourier transform infrared spectrometer was used to acquire the lasing spectral characteristics.

Narrow-ridge devices fabricated from wafer R066 had two significantly different etch depths, about 8 $\mu$m (denoted as deep etched) and 2 $\mu$m (denoted as shallow etched). A 14-$\mu$m-wide and 1-mm-long deep etched device operated at temperatures up to 213 K in cw mode and up to 280 K in pulsed mode, exhibiting unpredicted current-voltage characteristics as well as a wide wavelength tuning range at 80 and 100 K in cw mode, as shown in Fig. 2. At 80 K, the lasing wavelength was tunable by 230 $cm^{-1}$ (wavenumber) from 4.43 $\mu$m near

TABLE I. Active region structures for tunable IC lasers, and their tuning ranges and rates.

| Active QW design | Wafer | Active region Thickness in Å InAs/GaInSb/InAs (/GaInSb/InAs) | No. of stages | λ in μm at 80 K | Device size | | T(K) | cw/ pulse | Tuning range $cm^{-1}$ | Tuning rate $cm^{-1}/(A/cm^2)$ | Tuning rate $cm^{-1}/mA$ | Maximum current mA |
|---|---|---|---|---|---|---|---|---|---|---|---|---|
| | | | | | width μm | length mm | | | | | | |
| Two InAs QW layers | R066 | 24/29/21 | 12 | 4.43 | 14 | 1.0 | 80 | cw | 230 | -0.15 | -1.1 | 250 |
| | | | | | | | 100 | cw | 280 | -0.17 | -1.2 | 260 |
| | | | | | | 2.0 | 100 | cw | 74 | -0.073 | -0.26 | 250 |
| | | | | | | | | pulse | 90 | -0.020 | -0.071 | 1500 |
| | R084 | 22/29/21 | 8 | 4.35 | 150 | 1.5 | 120 | cw | 150 | -1.1 | -0.50 | 500 |
| | R089 | 22/29/23 | | 4.73 | | 0.75 | 180 | cw | 47 | -0.13 | -0.11 | 500 |
| | R090 | 22/29/21/**29** | | 4.76 | | 0.75 | 160 | cw | 51 | -0.13 | -0.12 | 500 |
| Three InAs QW layers | R064 | 28/33/25/**36/21** | 15 | 6.67 | 15 | 1.8 | 80 | cw | 180 | -0.13 | -0.49 | 360 |
| | | | | | 40 | 1.8 | 80 | cw | 100 | -0.16 | -0.22 | 500 |
| | | | | | | | 80 | pulse | 85 | -0.10 | -0.14 | 500 |
| | R094 | | | 6.89 | 20 | 3.0 | 80 | cw | 130 | -0.20 | -0.34 | 400 |
| | | | | | | | 80 | pulse | 99 | -0.13 | -0.22 | 450 |

the threshold current of 1.2 mA to 4.93 $\mu$m at 250 mA; while at 100 K, the lasing wavelength was tunable by about 280 $cm^{-1}$, from 4.47 to 5.10 $\mu$m when the current increased from 2.2 to 260 mA. The tuning range of 280 $cm^{-1}$ corresponds to an energy change ($\Delta E$) of 34.3 meV or a wavelength shift ($\Delta\lambda$) of 630 nm, which, to our knowledge, is the largest current tuning range achieved in a simple monolithically fabricated Fabry-Perot mid-IR laser. The threshold current density of this laser was 8.6 $A/cm^2$ at 80 K, which was very similar to values obtained for other lasers fabricated from the same and related wafers. However, the threshold voltage of this laser operated at 80 K exhibited a slightly higher value of 3.75 V (voltage efficiency of 90%) than typical values (3.51–3.68 V) for other devices made in the same processing batch from the same wafer R066. This may indicate a relatively large electric field across the active regions of this laser, so that the electron wave-function might be distributed more on the right-side InAs layer (Fig. 1(b)) for such a biasing voltage. As shown in Fig. 2(b), with further current increase, the operating voltage increased considerably to 4.97 V at 120 mA and then decreased slightly with additional current increase, instead of being pinned at the threshold value. Consequently, extra electric field was applied across the active regions that caused a red shift of the lasing wavelength, as suggested by Eq. (1). The wavelength tuning rate was relatively small at low currents and then increased strongly at higher currents, as shown in Fig. 2(b). This increase is partially due to an additional thermal contribution. The average tuning rate was $-0.15\,cm^{-1}/(A/cm^2)$ ($-1.07\,cm^{-1}/mA$) at 80 K and $-0.17\,cm^{-1}/(A/cm^2)$ ($-1.23\,cm^{-1}/mA$) at 100 K. The use of two units for the tuning rate is because the heating effect is better described in terms of $cm^{-1}/mA$, while Stark effect is better described with $cm^{-1}/(A/cm^2)$. The slight decrease in operating voltage above 120 mA could be caused by combined effects of Joule heating and decreased series resistance at high currents and is not necessarily indicative of a reduced electric field across active regions. This decrease of operation voltage was not observed for other devices made from the same wafer.

However, the current-tuned red-shift was observed from other devices that were fabricated from the same wafer. Figure 3 shows lasing spectra at various injection currents for another deep etched laser (14 $\mu$m × 2 mm) also made from wafer R066, for both cw and pulsed (1-$\mu$s pulse width, 5-kHz repetition rate) conditions at 100 K. An average tuning rate of $-0.073\,cm^{-1}/(A/cm^2)$ ($-0.26\,cm^{-1}/mA$) was observed from the laser at 100 K in cw operation and became $-0.10\,cm^{-1}/(A/cm^2)$ ($-0.36\,cm^{-1}/mA$) at 120 K (not shown here), which was smaller than the value of $-0.17\,cm^{-1}/(A/cm^2)$ ($-1.23\,cm^{-1}/mA$) obtained from the device in Fig. 2. This laser had a lower threshold voltage (3.63 V at 100 K) and the operating voltage consistently increased with the current. In pulsed operation, the red shift was initially very small and the tuning rate was about $-0.02\,cm^{-1}/(A/cm^2)$ ($-0.071\,cm^{-1}/mA$) with a range of about 90 $cm^{-1}$ for a large current up to 1.5 A. This pulsed-operation tuning rate is significantly lower than that for cw operation, suggesting that heating may have played an important role in the red-shift tuning for cw operation. For the shallow etched devices, red-shift tuning was also observed in cw operation, but with an about 20% smaller tuning range. This indicates that the heating effect was more significant in deep etched devices. In order to reduce the heating effect, only shallow etched devices (etch depth: 2 ~ 3 $\mu$m) were fabricated from other wafers.

To examine the behavior described by Eq. (1), wafers R084, R089, and R090 were designed with a narrower left-side InAs layer thickness, in contrast to R066, so that the electron wave-function will be pushed more to the right-side InAs layer for low-voltage operation. Broad-area devices made from wafer R084 lased at temperatures up to 180 K in cw mode (320 K in pulsed) with a lasing wavelength from 4.35 $\mu$m at 80 K to 5.1 $\mu$m at 300 K. These lasers had low threshold current densities (e.g., 4.5 $A/cm^2$ with a threshold

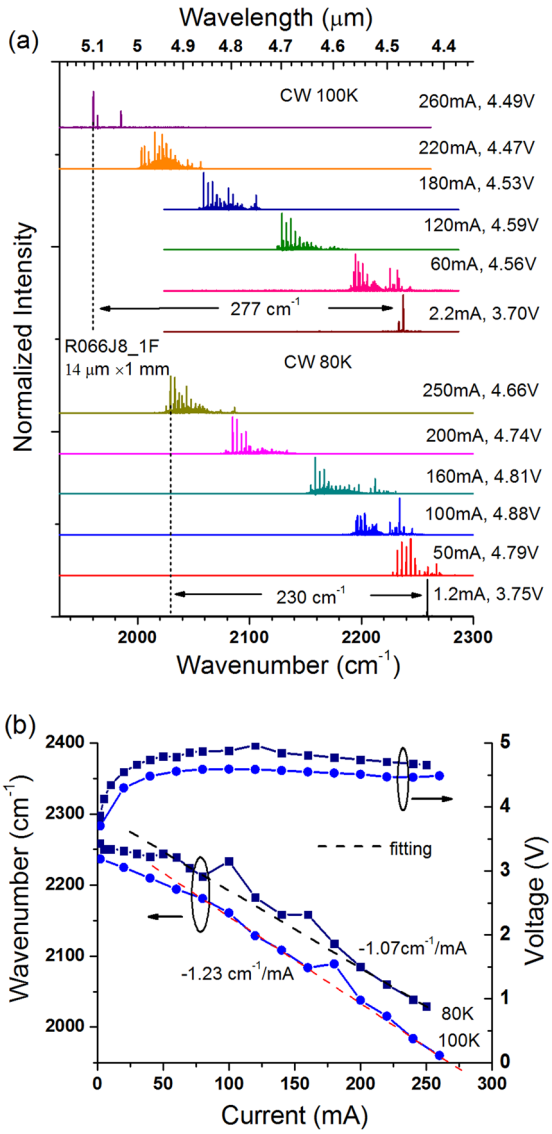


FIG. 2. (a) CW lasing spectra of a laser (14 $\mu$m × 1 mm) from R066 at 80 K and 100 K for various currents; (b) Operating voltage and lasing wavelength vs. current. The average tuning rates obtained by the fitting curves (dashed line) are $-1.07\,\mathrm{cm}^{-1}$/mA at 80 K and $-1.23\,\mathrm{cm}^{-1}$/mA at 100 K.

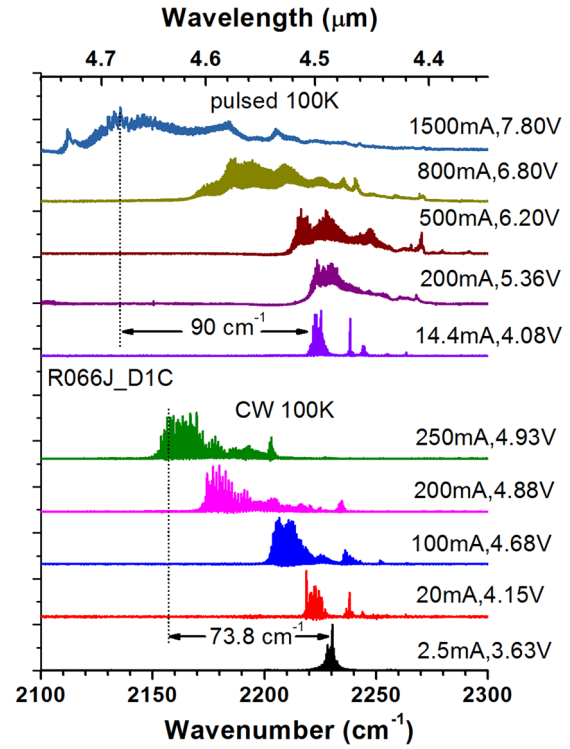


FIG. 3. Lasing spectra of an IC laser (14 $\mu$m × 2 mm) from R066 at 100 K for pulsed (upper) and CW (lower) conditions.

voltage of 2.8 V) and adequate output powers (e.g., ~162 mW/facet at 600 mA, an underestimate not including the correction due to the beam divergence) at 80 K. Figure 4 illustrates the lasing spectral characteristics of a broad-area device (150 $\mu$m × 1.48 mm) fabricated from wafer R084 in cw operation at 120 K for different currents (Fig. 4(a)), and how its lasing wavelength and operating voltage changed at five different temperatures from 100 to 180 K (Fig. 4(b)). The lasing wavelength tuning rate is small for low currents at low temperatures and increases rapidly for high currents at high temperatures. At 120 K, the wavelength was red-shifted over a range of 151 $\mathrm{cm}^{-1}$ with a tuning rate of $-1.1\,\mathrm{cm}^{-1}/(\mathrm{A/cm}^2)$ ($-0.5\,\mathrm{cm}^{-1}$/mA) at relatively high currents. However, in pulsed operation, the lasing wavelength was nearly unchanged with current. This probably indicated that the lasing red-shift observed in cw operation was mainly due to heating.

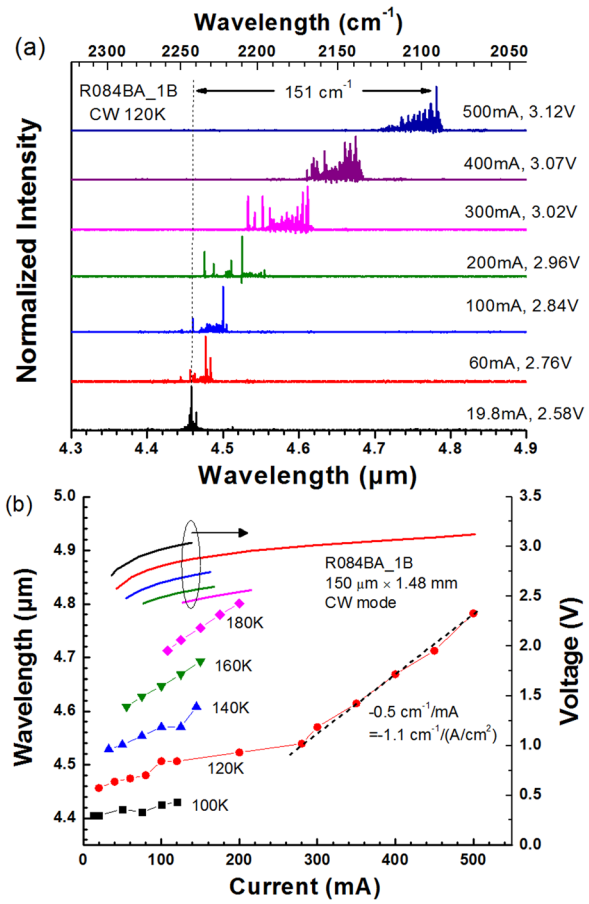


FIG. 4. (a) CW lasing spectra of a broad−area laser from R084 (150 $\mu$m × 1.48 mm) at 120 K for various currents; (b) Operating voltage and lasing wavelength vs. current at several temperatures.

Additionally, the narrow-ridge ($15\,\mu m \times 2\,mm$) laser from the same wafer red shifted at the much lower rate of $-0.039\,cm^{-1}/(A/cm^2)$ ($-0.13\,cm^{-1}/mA$) in cw mode and $-0.012\,cm^{-1}/(A/cm^2)$ ($-0.04\,cm^{-1}/mA$) in pulsed mode at 160 K with current up to 500 mA. The reduced tuning rate was probably due to the better heat dissipation in the narrow ridge laser device, supporting the implication of the heating effect mentioned earlier on the lasing red-shift with current in cw operation. In contrast, for laser devices in which the electron wave-function was designed to be mainly on the left InAs QW in the active region, the lasing wavelength was nearly unchanged with current in cw operation. Furthermore, the wavelength shift due to the temperature increase with current based on the extracted thermal resistance is considerably smaller than the observed tuning range. For example, the lasing wavelength of the broad-area laser at 120 K was shifted by 129 nm (Fig. 4(b)) when the current was increased from 280 to 400 mA, which is significantly larger than the estimated heating-induced shift of 50 nm (contributing ~39% in this increment) based on an extracted thermal resistance of 54 K/W and a temperature tuning coefficient of 3.4 nm/K. Also, Joule heating alone will not cause the abrupt change of tuning rate shown in Fig. 4. Such a change should be indicative of an adjustment of electron distribution over the active region related to the Stark effect. Hence, the large lasing red shift is caused by combined contributions of the Stark effect associated with specific QW structures, discussed above, and the heating effect.

Broad-area devices made from wafer R089 lased at temperatures up to 212 K near 5.25 $\mu$m (4.73 $\mu$m at 80 K) in cw mode and up to 270 K in pulsed mode near 5.42 $\mu$m. At 80 K, the threshold current density was 9.3 A/cm$^2$ and the output power exceeded 120 mW/facet at 700 mA. The broad-area devices made from wafer R090 lased at temperatures up to 185 K near 5.15 $\mu$m (4.76 $\mu$m at 80 K) in cw mode and 257 K in pulsed mode near 5.3 $\mu$m. Their overall performance was worse than that of the devices made from wafer R084 in threshold current density, cw output power, and maximum pulsed operating temperature. Narrow-ridge devices were also made from both wafers. A narrow-ridge ($10\,\mu m \times 1.7\,mm$) laser from wafer R089 lased at temperatures up to 253 K near 5.36 $\mu$m in cw mode and up to 280 K in pulsed mode near 5.48 $\mu$m, while a narrow-ridge ($15\,\mu m \times 1.5\,mm$) laser from wafer R090 lased at temperatures up to 228 K near 5.17 $\mu$m in cw mode and up to 257 K in pulsed mode near 5.29 $\mu$m.

In cw operation, the lasing wavelengths of all devices made from R089 and R090 exhibited large red-shifts with current, as shown in Fig. 5. At 180 K, the lasing wavelength was shifted by 46.7 cm$^{-1}$ for a broad area device from R089 with a tuning rate of about $-0.11\,cm^{-1}/mA$. At 160 K, a shift of 51 cm$^{-1}$ was observed for a broad area laser from wafer R090 with a tuning rate of $-0.12\,cm^{-1}/mA$. The tuning rates of devices made from wafers R089 and R090 were lower compared with the devices fabricated from wafer R084, as shown in Fig. 4. This is because these devices had improved thermal dissipation due to better mounting as evidenced by their higher cw operating temperatures, although their maximum pulsed operating temperatures were lower than those in devices from R084. Enhanced tuning rate with a wider range could

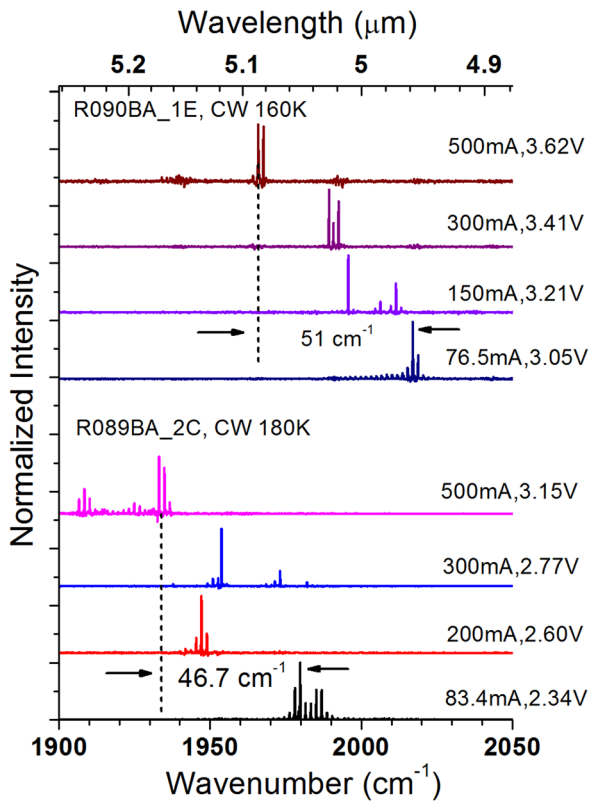


FIG. 5. Lasing spectra of broad-area IC lasers ($150\,\mu m \times 0.75\,mm$) from R089 at 180 K and R090 at 160 K, both for CW conditions.

be achieved with a high thermal resistance at a price of a reduced cw operating temperature. In pulsed operation, a red-shift with current was essentially not observed from devices made from either wafer. The results also indicated that the additional $Ga_{0.7}In_{0.3}Sb$ hole QW layer in the active region (R090) did not have any substantial impact on the wavelength tuning. This suggests that the tuning mechanism in these IC lasers could be different from what was in "collection QWs" or "charge accumulation layers."[14,21]

The tuning rates and ranges are summarized in Table I for representative devices made from all the wafers. Again, two units are used for the tuning rate to better represent Stark and heating effects, which is particularly meaningful for comparisons between devices of different size. As shown in the table, devices made from R066 exhibited tuning ranges and rates that are larger than those from other wafers at a similar wavelength. This is in contradiction with the theoretically calculated results based on the Stark effect (see Fig. 6) and may be the result of subtleties associated with device fabrication. Actually, the Stark effect, alone, would not usually result in lasing wavelength tuning. This is because in an ideal semiconductor laser, carrier concentration is pinned at the threshold and thus the lasing wavelength will not shift with further increase of injection current above threshold. Therefore, even if the electroluminescent emission can be tuned largely by the Stark effect in cascade emitting devices,[16,19] it is unlikely for the above-threshold lasing wavelength shift to be based exclusively on the Stark effect.

To unclamp the pinning of the carrier concentration, techniques to "slow down" lasing[20] that allow continued increase of

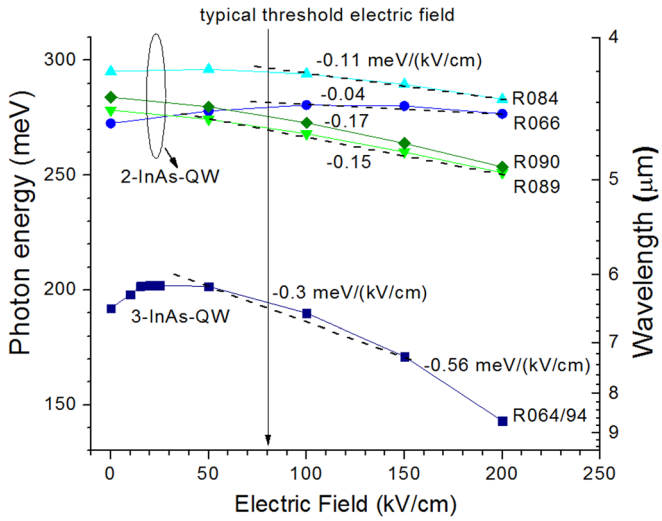


FIG. 6. The calculated interband transition energy and tuning rate for several 2-InAs-QW laser designs (R066, R084, R089, and R090) and a 3-InAs-QW laser design (R064/R094). A typical threshold electric field (80 kV/cm) is indicated by the arrow.

voltage across the active region were investigated. For QC lasers, a coupling state is inserted between the injection region and active region.[20] As a result, the electron transit across the active region was delayed allowing the increase in applied voltage after lasing. For interband lasers, the so-called "collection quantum wells"[21] or "charge accumulation layers"[14] were introduced via the insertion of a thick tunneling barrier, so that carriers are accumulated before recombining in the active region, leading to some increase of the voltage across the active region. For the above four IC laser structures, substantial red-shifts of lasing wavelengths were observed in cw operation, while the shift was either small or essentially zero in pulsed operation. This seems to suggest that the heating effect unlocks the carrier concentration pinning at the threshold, and then the Stark effect provides positive feedback that significantly enhances the red-shift of the lasing wavelength, as both effects have the same direction of wavelength shift. This is distinctively different from previous IC laser structures with electron wave-functions located mainly on the left-side InAs QW,[10–12,14] where the heating and Stark shift the wavelength in opposite directions.

On the other hand, real semiconductor lasers are not ideal and their carrier concentrations will not necessarily be pinned at the threshold. A non-pining of the carrier density above threshold was observed in previous IC lasers particularly at high temperatures.[22] Practically, the non-ideal conditions such as low tunneling efficiency and additional transition states may slow down the lasing process and result in a wavelength shift after lasing. Below, we will present IC lasers with three InAs QW layers in the active region, which exhibited substantial wavelength tuning even for pulsed conditions without heating.

### B. IC lasers with three InAs QW layers in the active region

In the past, multiple coupled QWs were found to have a more significant Stark effect in comparison with a single QW.[23,24] In our study, the multi-QW active region with three InAs QWs was introduced initially in IC lasers for different motivations. Two wafers, R064 and R094, with a nominally identical IC laser structure were grown separated by more than one year, to verify the reproducibility. The injection region and waveguide structure (with 15 cascade stages) are similar to the IC structure without the top semiconductor cladding layer in Ref. 18. The active region consists of InAs/GaInSb/InAs/GaInSb/InAs QW layers with thicknesses of 28/33/25/36/21 (in Å from left to right), in which one more pair of InAs and GaInSb QW was added compared to the W-like active region.

The calculated carrier distributions are depicted in Fig. 7 in the active region for three different electric fields.

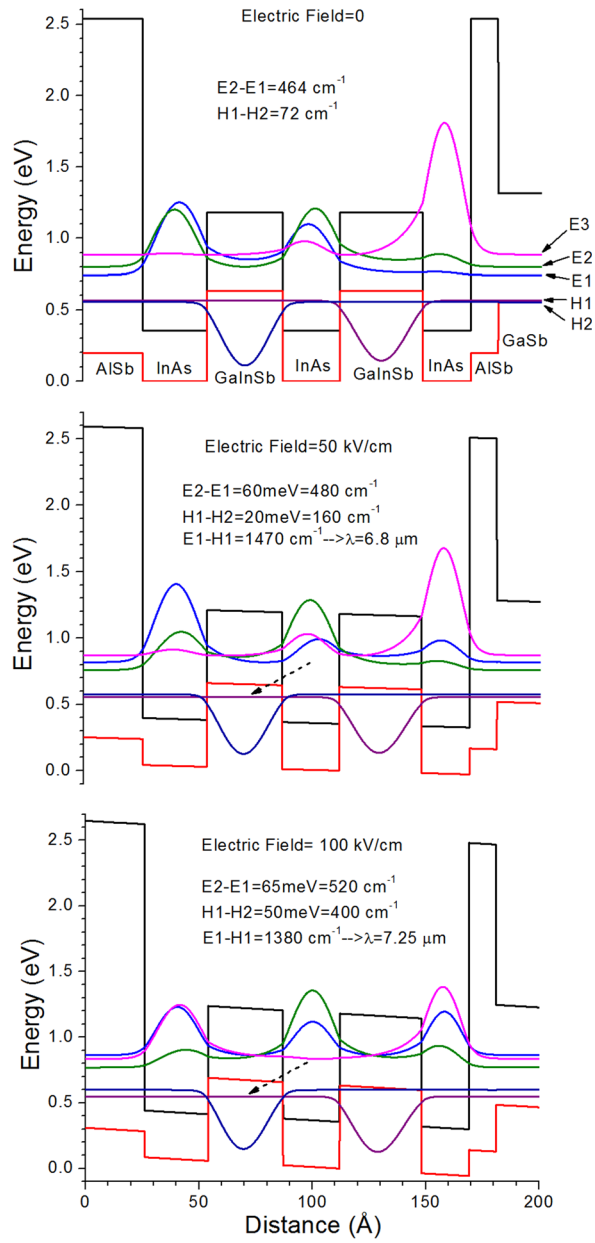


FIG. 7. Carrier distributions in the active region for structure R064 at various electric fields. Three lowest eigen energy levels for electron are labeled E1, E2, and E3; two lowest eigen energy levels for heavy hole are labeled H1 and H2. The energy separations between excited state and ground state are given in the graph. The interband transition is indicated by the dashed arrow and the corresponding lasing wavelength is also given.

Without an electric field applied, the two heavy-hole states have very similar energies, while the electron ground-state resides mainly in the left InAs QW. When an electric field is applied with an external forward bias on the device, the electron ground-state quickly moves to the middle InAs QW and the heavy-hole ground-state shifts to the left GaInSb QW, resulting in a positive value of ($z_e$-$z_h$). The resulting interband transition for lasing is indicated by the dashed arrow. As the electric field continues to increase, the energy separation between the two heavy-hole states becomes larger and the lasing transition will probably only occur between the electron and heavy-hole ground states with a further positive value of ($z_e$-$z_h$). As such, the Stark effect will result in an emission wavelength red shift with the electric field.

In Figure 6, the calculated interband transition energies as a function of the electric field for the 3-InAs-QW and 2-InAs-QW structures are compared to one another. The calculation shows a larger shift for the 3-InAs-QW design after the external field exceeds the typical threshold value. This is because the electron wave-function is extended further to the right-hand side with an additional InAs layer in the active region (see Fig. 7), while the ground hole state remains mostly on the left GaInSb QW layer, resulting in a much larger value for the interband dipole ($z_e$-$z_h$). Consequently, the red-shift of emission wavelength should be enhanced significantly according to Eq. (1) in the 3-InAs QW design compared to that in the 2-InAs-QW design.

The narrow-ridge lasers (without the top thick gold layer and coating) made from R064 lased at temperatures up to 188 K in cw mode, and up to 200 K in pulsed mode, respectively, with an emission wavelength up to 7.6 $\mu$m (6.7 $\mu$m at 80 K). The observed lasing wavelength was in good agreement with the calculated value, as shown in Fig. 6. The device performance was significantly improved compared to previous results from early InAs-based IC lasers at a similar wavelength.[25] Figure 8 shows the cw *L-I-V* characteristics of a 20 -$\mu$m-wide and 2.1-mm-long IC laser at various operating temperatures. The output power exceeded 22 mW/facet, and the threshold current density was 10 A/cm$^2$ at 80 K. However, the threshold current density of this device increased relatively quickly with increasing temperature. The characteristic temperature ($T_0$) of 30.5 K is lower than the typical value (>40 K) for an IC laser based on a 2-InAs-QW active region.[18] This may be due to the ~~reduced wave-function overlap between the two interband transition states in the 3-InAs-QW active region~~ and a lasing wavelength at the longer wavelength.

To investigate the electrical tuning properties of the 3-InAs-QW structure, lasing spectra of the IC lasers for different injection currents were collected at different heat-sink temperatures. Figure 9 shows a series of cw lasing spectra from a 15 -$\mu$m-wide laser at 80 K for injection current increasing from 2.2 to 360 mA and corresponding bias voltage from 3.6 to 6.7 V, respectively. In this electrical injection range, the lasing wavelength red-shifted by about 180 cm$^{-1}$ (22 meV or 900 nm) with a tuning rate of −0.49 cm$^{-1}$/mA. The tuning range covers over 12.5% of the center emission wavelength, indicating significant electrical tuning for such a

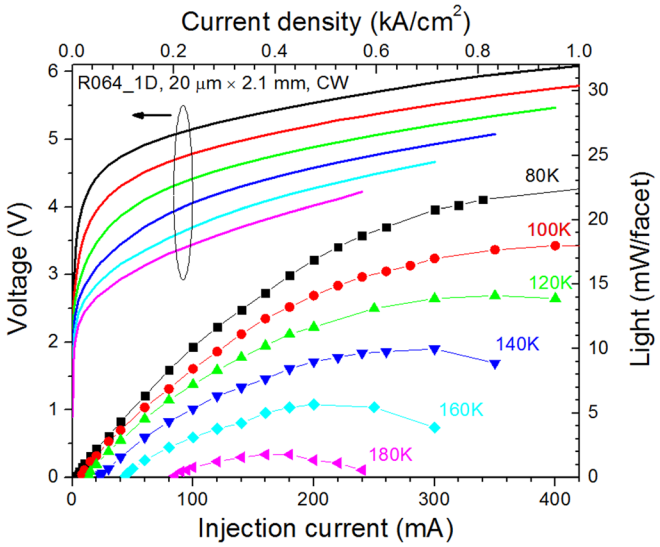


FIG. 8. Light-current-voltage characteristics of an IC laser (20 $\mu$m × 2.1 mm) from R064 at different heat-sink temperatures in CW mode.

laser structure. To examine the contribution of the heating effect, the lasing spectra of a 40 -$\mu$m-wide ridge device were measured at 80 K in cw and pulsed (0.5 $\mu$s pulse width at 1 kHz repetition rate) modes, as shown in Figure 10. The tuning span observed in cw mode is 100 cm$^{-1}$ (13 meV) from this device, compared to 85 cm$^{-1}$ (11 meV) in pulsed mode (same maximum current up to 500 mA). This indicates that the wavelength shift was mainly due to the Stark effect. Lasing wavelengths of six other devices with different ridge width sizes (15–40 $\mu$m-wide) were also examined at 80 K. It was found that they have similar red-shifts versus the injection current density (average tuning coefficient of ~0.13 cm$^{-1}$/ (A/cm$^2$)).

Both narrow-ridge and broad-area devices made from wafer R094 were also investigated. These devices had threshold current densities of 10–14 A/cm$^2$ at 80 K, which are comparable to devices from R064. They all exhibited substantial red-shifts with increasing injection current in

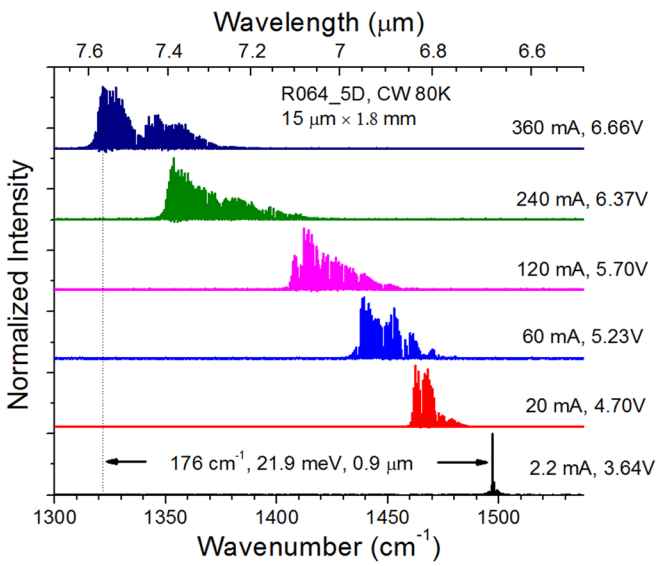


FIG. 9. CW lasing spectra of an IC laser (15 $\mu$m × 1.8 mm) from R064 at 80 K for various currents.

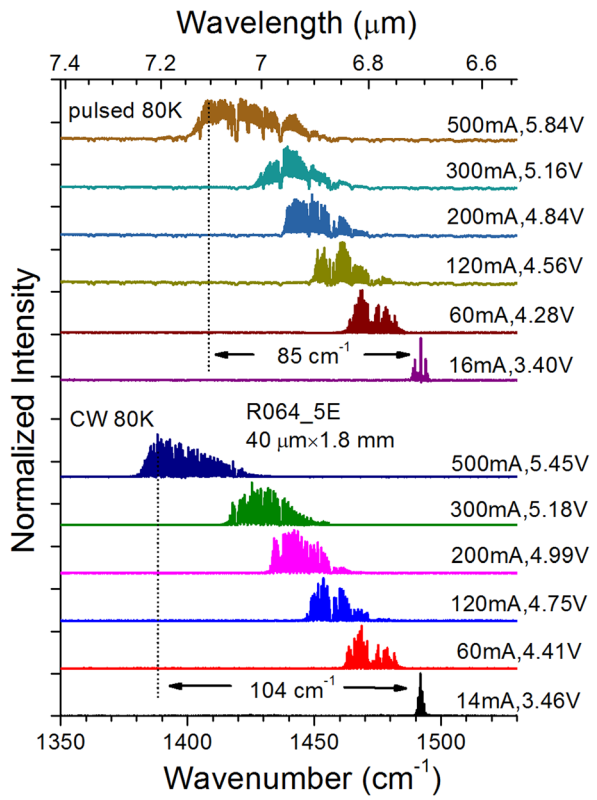


FIG. 10. Lasing spectra of an IC laser (40 $\mu$m × 1.8 mm) for various injection conditions in both CW and pulsed modes.

both cw and pulsed modes. For example, a 20-$\mu$m-wide and 3-mm-long IC laser at 80 K had a lasing wavelength red-shift of 132 $cm^{-1}$ in cw mode and 99 $cm^{-1}$ in pulsed mode when current was increased from 8 mA to 450 mA. This verifies that the "3-InAs-QW" structure is very promising and effectively unclamps the carrier concentration pinning, leading to significant current tuning of the lasing wavelength associated with a large value of the dipole ($z_e$-$z_h$) for enhanced Stark effect. This might be attributed to more substantial electron wave-function spreading into the multiple QWs and a consequent reduction in wave-function overlap with the localized hole state, resulting in an effective "slow down" of the lasing process, as mentioned previously. The large dipole ($z_e$-$z_h$) for the enhanced linear Stark effect in the 3-InAs QW configuration leads to a strong electrical tuning in a wide range, at a cost of possibly higher threshold current density and reduced maximum operating temperature compared to the 2-InAs QW configuration.

## III. CONCLUDING REMARKS

In summary, electrically tunable interband cascade lasers were demonstrated with a wide tuning span of about 280 $cm^{-1}$ (34 meV or 630 nm) near 4.5 $\mu$m and about 180 $cm^{-1}$ (22 meV or 900 nm) near 7 $\mu$m. The wide wavelength tuning was achieved by making the Stark effect wavelength shift in the same direction as the wavelength shift due to the heating effect with current injection. As such, both effects provided positive feedback to each other to enhance the lasing red-shift with electrical current. This mutually enhancing Stark and heating effects may also be applied to QC lasers, allowing a strongly tuned red-shift instead of the usual blue shift[2,7,8] used up to now. Furthermore, by comparing the 3-InAs-QW and 2-InAs-QW active region designs, we demonstrated how a strong electrical tuning with a large range can be achieved in both cw and pulsed modes through adjusting the electron wave-function and the interband dipole. This may open up a new way to optimize the electrical tuning of lasers.

## ACKNOWLEDGMENTS

The authors thank J. C. Keay and C. Niu for technical assistance. This work was supported in part by the National Science Foundation (ECCS-1002202), and by C-SPIN, the Oklahoma/Arkansas MRSEC (DMR-0520550). K. Mansour was supported by NASA Planetary Instrument Definition & Development Program.

[1]K. Wörle, F. Seichter, A. Wilk, C. Armacost, T. Day, M. Godejohann, U. Wachter, J. Vogt, P. Radermacher, and B. Mizaikoff, "Breath analysis with broadly tunable quantum cascade lasers," Anal. Chem. **85**, 2697–2702 (2013).
[2]J. Faist, F. Capasso, C. Sirtori, D. L. Sivco, A. L. Hutchinson, and A. Y. Cho, "Laser action by tuning the oscillator strength," Nature **387**, 777–782 (1997).
[3]J. Faist, C. Gmachl, F. Capasso, C. Sirtori, D. L. Sivco, J. N. Baillargeon, and A. Y. Cho, "Distributed feedback quantum cascade lasers," Appl. Phys. Lett. **70**, 2670–2672 (1997).
[4]A. Muller, M. Beck, J. Faist, U. Oesterle, and M. Ilegems, "Electrically tunable, room-temperature quantum-cascade lasers," Appl. Phys. Lett. **75**, 1509–1511 (1999).
[5]C. Gmachl, D. L. Sivco, R. Colombelli, F. Capasso, and A. Y. Cho, "Ultra-broadband semiconductor laser," Nature **415**, 883–887 (2002).
[6]A. Mohan, A. Wittmann, A. Hugi, S. Blaser, M. Giovannini, and J. Faist, "Room-temperature continuous-wave operation of an external-cavity quantum cascade laser," Opt. Lett. **32**, 2792–2794 (2007).
[7]Y. Yao, Z. Liu, A. J. Hoffman, K. J. Franz, and C. F. Gmachl, "Voltage tunability of quantum cascade lasers," IEEE J. Quantum Electron. **45**, 730–736 (2009).
[8]A. Bismuto, R. Terazzi, M. Beck, and J. Faist, "Electrically tunable, high performance quantum cascade laser," Appl. Phys. Lett. **96**, 141105-3 (2010).
[9]R. Q. Yang, "Infrared laser based on intersubband transitions in quantum wells," Superlattices Microstruct. **17**, 77–83 (1995).
[10]I. Vurgaftman, W. W. Bewley, C. L. Canedy, K. Chul Soo, K. Mijin, C. D. Merritt, J. Abell, and J. R. Meyer, "Interband cascade lasers with low threshold powers and high output powers," IEEE J. Select. Top. Quantum Electron. **19**, 1200210 (2013).
[11]R. Weih, M. Kamp, and S. Hofling, "Interband cascade lasers with room temperature threshold current densities below 100 A/$cm^2$," Appl. Phys. Lett. **102**, 231123-4 (2013).
[12]C. L. Canedy, W. W. Bewley, M. Kim, C. S. Kim, J. A. Nolde, D. C. Larrabee, J. R. Lindle, I. Vurgaftman, and J. R. Meyer, "High-temperature interband cascade lasers emitting at lambda = 3.6–4.3 $\mu$m," Appl. Phys. Lett. **90**, 181120-3 (2007).
[13]J. S. Yu, A. Evans, S. Slivken, S. R. Darvish, and M. Razeghi, "Short wavelength $\lambda \sim 4.3$ $\mu$m high-performance continuous-wave quantum-cascade lasers," IEEE Photon. Technol. Lett. **17**, 1154–1156 (2005).
[14]S. Suchalkin, M. V. Kisin, S. Luryi, G. Belenky, F. J. Towner, J. D. Bruno, C. Monroy, and R. L. Tober, "Widely tunable type-II interband cascade laser," Appl. Phys. Lett. **88**, 031103-3 (2006).
[15]J. R. Meyer, C. A. Hoffman, F. J. Bartoli, and L. R. Ram-Mohan, "Type-II quantum-well lasers for the mid-wavelength infrared," Appl. Phys. Lett. **67**, 757–759 (1995).
[16]R. Q. Yang, C.-H. Lin, S. J. Murry, S. S. Pei, H. C. Liu, M. Buchanan, and E. Dupont, "Interband cascade light emitting diodes in the 5–8 $\mu$m spectrum region," Appl. Phys. Lett. **70**, 2013–2015 (1997).
[17]R. Q. Yang and J. M. Xu, "Analysis of transmission in polytype interband tunneling heterostructures," J. Appl. Phys. **72**, 4714–4726 (1992).

[18]Z. Tian, Y. Jiang, L. Li, R. T. Hinkey, Z. Yin, R. Q. Yang, T. D. Mishima, M. B. Santos, and M. B. Johnson, "InAs-Based Mid-Infrared Interband Cascade Lasers Near 5.3 $\mu$m," IEEE J. Quantum Electron. **48**, 915–921 (2012).
[19]J. Faist, F. Capasso, C. Sirtori, D. Sivco, A. L. Hutchinson, S. N. G. Chu, and A. Y. Cho, "Midinfrared field-tunable intersubband electroluminescence at room-temperature by photon-assisted tunneling in coupled-quantum wells," Appl. Phys. Lett. **64**, 1144–1146 (1994).
[20]Y. Yao, K. J. Franz, X. Wang, J.-Y. Fan, and C. Gmachl, "A widely voltage-tunable quantum cascade laser based on "two-step" coupling," Appl. Phys. Lett. **95**, 021105-3 (2009).
[21]N. Le Thomas, N. T. Pelekanos, and Z. Hatzopoulos, "Tunable laser diodes by Stark effect," Appl. Phys. Lett. **83**, 1304–1306 (2003).
[22]B. A. Ikyo, I. P. Marko, A. R. Adams, S. J. Sweeney, C. L. Canedy, I. Vurgaftman, C. S. Kim, M. Kim, W. W. Bewley, and J. R. Meyer, "Temperature dependence of 4.1 $\mu$m mid-infrared type II "W" interband cascade lasers," Appl. Phys. Lett. **99**, 021102-3 (2011).
[23]W. L. Bloss, "Electric field dependence of the eigenstates of coupled quantum wells," J. Appl. Phys. **67**, 1421–1424 (1990).
[24]P. F. Yuh and K. L. Wang, "Large Stark effects for transitions from local states to global states in quantum well structures," IEEE J. Quantum Electron. **25**, 1671–1676 (1989).
[25]Z. Tian, R. Q. Yang, T. D. Mishima, M. B. Santos, and M. B. Johnson, "Plasmon-waveguide interband cascade lasers near 7.5$\mu$m," IEEE Photon. Technol. Lett. **21**, 1588–1590 (2009).